

## Microcantilever-Enabled Neutron Detection

<sup>1</sup>Kevin R. Kyle, <sup>1</sup>Michael J. Mendez, <sup>1</sup>Richard J. Venedam,  
<sup>2</sup>Timothy L. Porter

<sup>1</sup>National Security Technologies, LLC, 2621 Losee Rd, North Las Vegas, NV, 89030, USA

<sup>2</sup>University of Nevada Las Vegas, MS 4001, Las Vegas, NV, 89178, USA

<sup>2</sup>Tel.: 702 895 2058

<sup>2</sup>E-mail: [tim.porter@unlv.edu](mailto:tim.porter@unlv.edu)

Received: 10 February 2014 /Accepted: 7 April 2014 /Published: 30 April 2014

---

**Abstract:** A new concept for neutron radiation detection was demonstrated using piezoresistive microcantilevers as the active sensing element. Microcantilevers were used to measure the tiny volumetric changes in a sensing material upon absorption of neutron radiation and transmutation into a new element. Highly ordered inorganic crystalline lattices of boron-rich materials dispersed in polymeric rubber matrices were shown to act as volumetric neutron transducers. Copyright © 2014 IFSA Publishing, S. L.

**Keywords:** Neutron Detection, Microcantilever, Piezoresistive, Transmutation, Boron.

---

### 1. Introduction

The principal means of detecting the thermal neutron signature of fissile nuclear materials is a helium-3 (<sup>3</sup>He) gas detector, wherein absorption of neutrons forms charged particles that are then detected as a current in a gas-filled tube. This isotope of helium has a small natural abundance on earth, ( $1.38 \times 10^{-4}$ ) % [1]. The main source of <sup>3</sup>He for neutron detectors has been from the beta particle decay of tritium (<sup>3</sup>H), which at one time was manufactured in quantity for use in nuclear weapons. However, production of <sup>3</sup>H in the United States ceased in 1988 (U. S. Nuclear Regulatory Commission, 2009). With the current need for neutron detectors to detect and deter the smuggling of nuclear materials through ports and other border entry points into the United States, it is estimated that the demand for <sup>3</sup>He is 10 times the current worldwide supply [2]. However, plans to deploy neutron detectors to points of entry into the United States have halted, as viable alternatives

to <sup>3</sup>He neutron detectors are currently unavailable [3].

Boron-10 (<sup>10</sup>B) has a neutron absorption cross section (3838 barns) comparable to that of <sup>3</sup>He (5330 barns) [1]. And, the natural abundance of <sup>10</sup>B (19.8 %) is nearly six orders of magnitude greater than that of <sup>3</sup>He, making it an attractive alternative to <sup>3</sup>He. The absorption of thermal neutrons by <sup>10</sup>B produces a lithium atom (<sup>6</sup>Li, with energy of 0.84 MeV) and an alpha particle (α, 1.47 MeV). Gas-tube neutron detectors based on the gaseous boron compound BF<sub>3</sub> exist and operate on a principle similar to that of a <sup>3</sup>He detector. Solid boron materials have been used as moderators and absorbers of neutrons in reactors, as well as shielding in other neutron-producing devices. The use of solid, condensed-phase materials rich in boron (greater than 50 % by weight) for use as the active neutron absorber is attractive due to their greater density (neutron absorber per unit area), their chemical inertness, and their cheap commercial abundance over gas-phase materials.

Prior work has shown that solid materials consisting of highly ordered boron-rich lattices undergo morphological changes upon neutron irradiation [4-7]. Changes in volume, hardness, and physical integrity (fissuring) have been attributed to both the transmutation of boron atoms in a rigid lattice into lithium ions, which disrupts the chemical bonding and charge balance of the material, and the accumulation of helium within voids in the material. Additionally, lattice damage and concomitant material volume change occur due to the passage of these energetic ions through the material. The goal of this project was to exploit this neutron-induced volume change as a means of neutron detection. The means of transduction of this volume change into an easily detectable electronic response is a microcantilever.

## 2. Experimental Setup and Procedure

Microcantilever-based sensors may operate as static coated devices, vibrating cantilever devices, contact-mode devices, or embedded sensors [8-9]. Both piezoelectric (actively driven) and piezoresistive (passive readout) cantilevers have been demonstrated in various chemical-sensing applications. Embedded piezoresistive microcantilever (EPM) sensors provide a simple, low-cost, and effective platform for the detection of analytes [8-12]. In the EPM sensor, a piezoresistive microcantilever is embedded or partially embedded into a sensing material. An embedded microcantilever is in contact with a much greater volume of sensing material compared to a microcantilever sensor based on a thin coating on the cantilever itself. This is important in radiation sensing because it provides a much greater interaction volume for the radiation to be detected. The sensing material can be a polymer, composite polymer, or inorganic material that acts as a probe for the desired analyte. Upon analyte exposure, reactions within the sensor probe material result in a volumetric change, which is measured as a resistance change within the piezoresistive microcantilever due to a change in bending strain. This volumetric shift in the sensing material may be due to diffusion of the analyte into the sensing material, probe-target binding on the material surface or in the bulk, or surface or bulk chemical reactions between the analyte and sensing material. The latter interaction is representative of radiation sensing, wherein ions produced in the sensing material result in molar volume changes due to the bond breaking in the crystalline lattice structure, electronic repulsions, and lattice damage due to deposition of excess energy. Any swelling or contraction of the material in contact with the cantilever tip results in an immediate, easily measurable change in the cantilever channel resistance. This change is in linear proportion to the amount of the material swelling; therefore, a simple ohmmeter circuit is

sufficient to record the sensing activity. Cantilever strains of only a few angstroms are measurable. The simplicity of the EPM readout circuitry allows for small size and long-life battery operation.

Sensor Scientific was contracted to supply the microcantilever sensors utilized in this project. The microcantilevers, contained in a die, are approximately 200 microns long and 40 microns wide (Fig. 1a). The nominal resistance of an unstrained cantilever is approximately 2.2 k $\Omega$ . Each cantilever extends into a small circular area on the die in order to contain the sensing material. The sensing material was applied as a bead of organic liquid solution onto the die; the resulting polymeric drop coated the microcantilever (Fig. 1b).

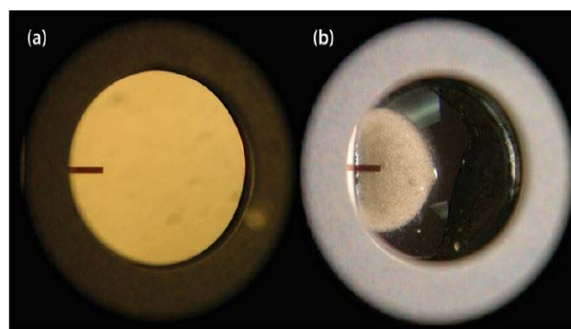


**Fig. 1.** (a) Bare microcantilever in a elliptical metal die; (b) microcantilever embedded in a dispersion of  $^{11}\text{B}$  $^{13}\text{C}$  in polydimethylsiloxane (PDMS).

In addition, each cantilever die also contains an integrated thermistor if temperature correction is needed. The entire cantilever was packaged on a printed circuit board with a mini-SD-type connector (Fig. 2). For the neutron detection experiments, an Agilent 34410A 6 1/2 digit datalogging multimeter was used to directly measure the cantilever or thermistor resistance as a function of time.

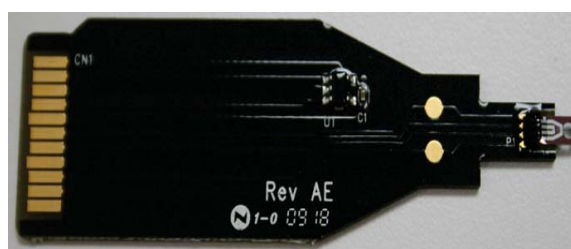


**Fig. 2.** Fully assembled microcantilever with a standard SD connector.

The criteria used for selecting boron materials were (1) a high (>50 %) boron content for efficient neutron absorption; (2) a rigid, highly ordered crystal structure; (3) low-cost commercial availability; and (4) low chemical reactivity. The metal hexaborides were prime candidates. Calcium and lanthanum

hexaboride ( $MB_6$ ,  $M = Ca, La$ ) are available from Aldrich Chemical as natural abundance boron (19.8 %  $^{10}B$ , 90.2 %  $^{11}B$ ), fine-mesh crystalline powders. The compounds consist of highly ordered covalently bonded octahedra of  $B_6^{2-}$  linked in a three-dimensional (3-D) network via B-B bonds, with the metal counter-ion located at the octahedral center of symmetry. Prior work on neutron irradiation of these metal borides demonstrated the large degree of physical change induced by the transmutation of boron into lithium and a, wherein expansion of physical dimensions, fissuring, hardness, and changes in chemical bonding as reflected in x-ray diffraction patterns were reported [5-7]. Natural-abundance boron nitride (BN) was also used due to its ubiquitous low-cost commercial availability.

Boron compounds enriched as either  $^{10}B$  or  $^{11}B$  were procured from Ceradyne Boron Products, LLC. Enrichment in these isotopes allows the decoupling of neutron-induced effects (in the  $^{10}B$ ) from background effects such as temperature and gamma-ray interactions, owing to the negligible neutron absorption by the  $^{11}B$  isotope (0.005 barns). Because the isotope-enriched metal hexaborides were unavailable, boron carbide ( $B_4C$ ) was purchased as both the 96 %  $^{10}B$  and 99+%  $^{11}B$  forms.  $B_4C$  also fit the selection criteria, consisting of well-ordered icosahedra of  $B_{12}$  covalently bonded to three carbons, and linked in a 3-D network via B-B and B-C-B bonds [13]. Prior work on neutron irradiation of  $B_4C$  demonstrated the large degree of physical change induced by neutron absorption (due to trapping of  $^4He$ ) and scission of B-C-B bonds [4, 14]. Coupling of the solid borides to the microcantilevers was accomplished via dispersion in a polymer rubber matrix, either polydimethylsiloxane (PDMS) or tert-butyl (tBu) rubber. Dispersions for tBu were prepared by dissolving the polymer in toluene or trichloroethylene, and adding 25 to 30 weight percent of the boride. Neutron irradiations were performed using a californium-252 ( $^{252}Cf$ ) neutron source. As the average neutron energy of this source is 2.1 MeV, a 1 inch thick, high-density polyethylene (HDPE) moderator was used to thermalize the neutrons (0.025 eV). The experimental setup is shown in Fig. 3.



Fig. 3. Experimental neutron setup.

The  $^{252}Cf$  source was placed outside of the HDPE enclosure. The EPM detectors were placed inside the enclosure. The HDPE functioned as a neutron energy moderator.

A summary of the polymer/rubber matrices used with the boron compounds integrated is shown in Table 1 below. Dispersions for tBu were prepared by dissolving the polymer in toluene or trichloroethylene, and adding 25 to 30 weight percent of the boride. The PDMS was a standard two-component system. Here, 25 to 30 weight percent was dispersed in the mixed compound. A 24-hour curing period was used prior to sensor assembly.

Table 1. Boron compounds used with the matrices tBu and PDMS.

Matrix				
tBu	CaB <sub>6</sub>	LaB <sub>6</sub>		
PDMS	CaB <sub>6</sub>	BN	$^{10}B_4C$	$^{11}B_4C$

The microcantilever sensors were assembled using a custom micromanipulator. Individual cantilevers were slowly brought into contact with the sensing materials using the micromanipulator, and pre-loaded to about 50  $\Omega$  resistance above their nominal, non-strained equilibrium value. The resulting assemblies were then epoxied into place and allowed to cure for 24-48 hours prior to use. A photo of the manipulator during the assembly process is shown in Fig. 4 below. Pre-loading of the microcantilever sensors allows for the sensors to form a single, rigid unit that is insensitive to most external vibrations and movement. In addition, the pre-loaded sensors may then respond in either of two directions (less resistance or greater resistance) equally.

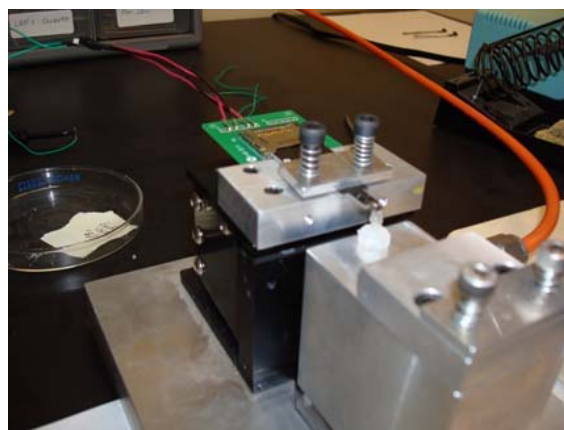


Fig. 4. Sensor micromanipulator assembly.

Individual cantilevers are slowly brought into contact with the sensing materials using the

micromanipulator, and pre-loaded to about 50  $\Omega$  resistance above their nominal, non-strained equilibrium value

### 3. Results and Discussion

The  $^{252}\text{Cf}$  was placed outside of a 1-inch-thick HDPE cylinder. The microcantilevers (up to three at a time) were placed on the inner wall of the cylinder for exposure to thermal neutrons. The microcantilever resistance was logged every five minutes using the Agilent datalogging multimeter. The neutron flux was measured by the gold foil technique, wherein a gold foil (sensitive to all neutrons) or a cadmium-shielded gold foil (epithermal neutrons only) was activated by neutron absorption, and the gamma counts were measured with a cooled germanium detector. The thermal neutron flux, calculated by subtracting the epithermal flux from the total flux, was measured to be 5.7 neutrons per  $\text{cm}^2\text{s}$ . This number translates to roughly 0.25 neutrons per second at the microcantilever, a number lower by three orders of magnitude than expected for this experiment. The consequence of the low neutron flux was null results in the chemical and physical characterizations of the effect of neutron absorption on our candidate materials. It also greatly enhanced the effect of the temperature background relative to the neutron effect. Fig. 5 shows the effect of temperature on a bare microcantilever over time. The microcantilever response correlates very well with the measured response on the built-in thermistor.

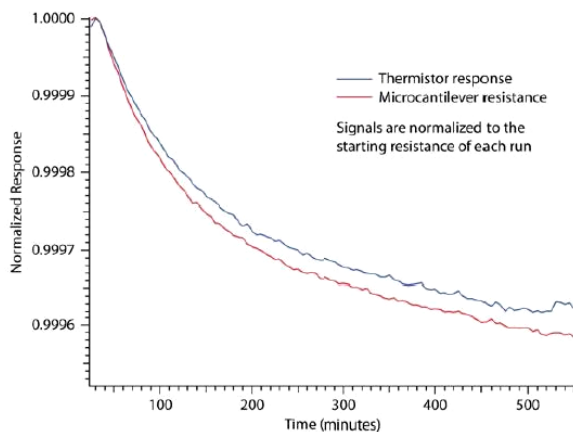


**Fig. 5.** Temperature response of a microcantilever device as measured by microcantilever resistance and on-board thermistor response shows the effect of temperature on the piezoresistance of the device.

The effect of neutron absorption on the microcantilevers can be seen in the comparison between  $^{10}\text{B}_4\text{C}$  and  $^{11}\text{B}_4\text{C}$  in PDMS shown in Fig. 6. The  $^{11}\text{B}$  trace is due solely to temperature drift in the neutron irradiation setup. The  $^{10}\text{B}$  trace exhibits a response that is counter to the downward

temperature drift. The response due to neutron absorption is shown as a positive response when corrected for temperature as shown in Fig. 7. Similarly, the response of boron lanthanum ( $\text{LaB}_6$ ) in tBu gives an increase in microcantilever resistance under neutron irradiation when corrected for temperature, as shown in Fig. 8.

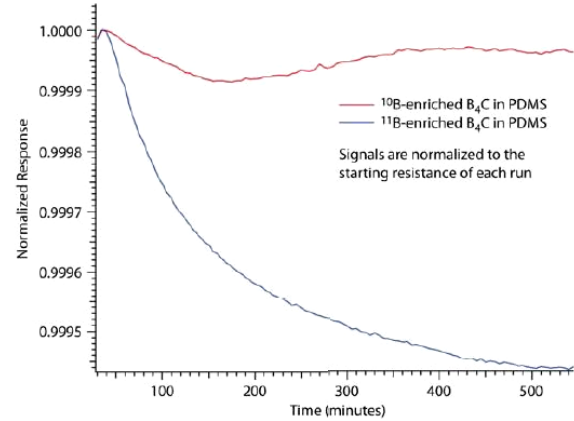


**Fig. 6.** Response of  $^{10}\text{B}$  and  $^{11}\text{B}$  boron carbide microcantilever devices to neutron irradiation indicates that the device is responsive to neutron absorption ( $^{10}\text{B}$ ) independent of the temperature effect ( $^{11}\text{B}$ ).

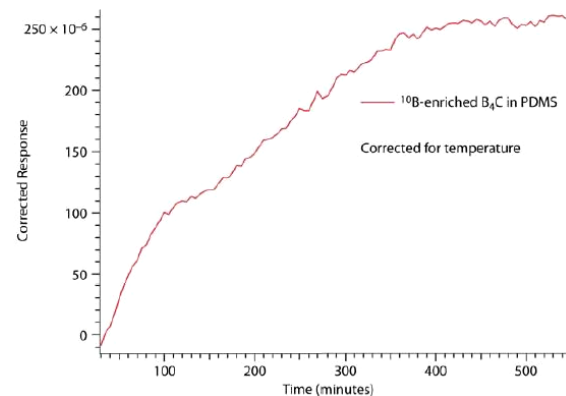


**Fig. 7.** Response of  $^{10}\text{B}$  boron carbide PDMS microcantilever devices to neutron irradiation, corrected for temperature, shows that the piezoresistance of the device increases as a result of neutron absorption over time.

Additional sensors tested included  $\text{CaB}_6$  in tBu,  $\text{CaB}_6$  in PDMS, and  $\text{BN}$  in PDMS. An increase in microcantilever resistance as a function of neutron irradiation was noted for each of these sensors. While the low neutron flux did not allow a more quantitative analysis due to the much greater temperature effect, the data do show that the detection of neutrons is possible using compound sensing materials composed of a polymer or rubber matrix with boron rich compounds interspersed within the matrix. Mechanical transduction using microcantilevers is a feasible means of detecting and measuring thermal neutrons using these compounds.

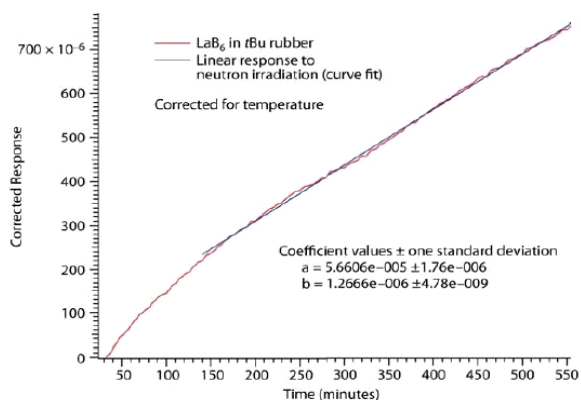


**Fig. 8.** Response of natural abundance  $\text{LaB}_6$  tBu rubber microcantilever device to neutron irradiation, which shows an increase in piezoresistance as a result of neutron absorption over time.

#### 4. Conclusions

A mechanical means of neutron detection was successfully demonstrated. Piezoresistive microcantilevers were shown to function as a means of detecting the change in volume in a boron-rich crystalline inorganic material upon absorption of a neutron and transmutation into a lithium ion and alpha particle. The boron-rich compounds were dispersed into a host matrix material comprised of either tBu or the polymer PDMS. As with all piezoresistive sensors fabricated in this fashion, the microcantilever resistance proved to be sensitive to temperature, requiring temperature monitoring using the integrated cantilever thermistors during the neutron absorption experiment and data correction afterward. Further research is required to quantify and calibrate the effect. Additional experiments with a higher-flux neutron source would allow the origin and magnitudes of the neutron-induced volume changes to be measured. Finally, research toward a reversible neutron transducer would allow the use of the microcantilever system as a reusable neutron detector.

#### Acknowledgements

We respectfully dedicate this paper to the memory of our friend and colleague Dr. Kevin Kyle. Support for this project was provided by National Security Technologies, LLC.

#### References

- [1]. G. Freidlander, J. W. Kennedy, E. S. Macias, J. M. Miller, Nuclear and Radiochemistry, 3 ed., John Wiley and Sons, New York, 1981.
- [2]. M. L. Wald, Shortage slows a program to detect nuclear bombs, 2009, [http://www.nytimes.com/2009/11/23/us/23helium.html?\\_r=28&partner=rss&mc=rss](http://www.nytimes.com/2009/11/23/us/23helium.html?_r=28&partner=rss&mc=rss)
- [3]. A. D. Snider, Subcommittee Investigates the Shrinking Global Supply of Helium-3, 2010, <http://science.house.gov/press/PRArticle>
- [4]. K. Froment, D. Gosset, M. Gary, B. Kryger, C. Verdeau, Neutron irradiation effects in boron carbides: Evolution of microstructure and thermal properties, *Journal of Nuclear Materials*, 188, 1992, pp. 185-188.
- [5]. M. S. Kovalchenko, V. V. Ogorodnikov, A. G. Krainii, Effect of neutron irradiation on the structure and properties of lanthanum hexaboride, *Atomic Energy*, 21, 6, 1966, pp. 1168-1174.
- [6]. V. V. Ogorodnikov, M. S. Kovalchenko, A. G. Krainii, Effect of neutron irradiation on the electrical resistance and color of high-melting compounds, *Powder Metallurgy and Ceramics*, 8, 5, 1969, pp. 411-414.
- [7]. T. Shikama, H. Kayano, Structural changes of deposited Ti<sub>1-x</sub>B<sub>x</sub> films due to neutron irradiation, *Journal of Nuclear Materials*, 179, 1991, pp. 465-468.
- [8]. T. L. Porter, M. P. Eastman, Microcantilever Sensor, *USA Patent 6,523,392*, 2003.
- [9]. T. L. Porter, M. P. Eastman, C. Macomber, W. G. Delinger, R. Zhine, An Embedded polymer piezoresistive microcantilever sensor, *Ultramicroscopy*, 97, 2003, pp. 365-369.
- [10]. A. Kooser, R. L. Gunter, W. G. Delinger, T. L. Porter, M. P. Eastman, Gas sensing using embedded piezoresistive microcantilever sensors, *Sensors and Actuators*, 99, 2-3, 2004, pp. 430-433.
- [11]. T. L. Porter, T. Vail, M. P. Eastman, R. Stewart, J. Reed, R. Venedam, *et al.*, A Solid-State sensor platform for the detection of hydrogen cyanide gas, *Sensors and Actuators*, 123, 2007, pp. 313-317.
- [12]. R. J. Venedam, Detection of chlorine gas, *Nevada Test Site-Directed Research and Development*, 1, 2009, pp. 185-190.
- [13]. F. Thevenot, Boron carbide - A comprehensive review, *Journal of the European Ceramic Society* 6, 4, 1990 pp. 205-225.
- [14]. D. Simeone, C. Mallet, P. Dubuisson, G. Baldinozzi, C. Gervais, J. Maquet, Study of boron carbide evolution under neutron irradiation by Raman spectroscopy, *Nuclear Materials*, 277, 1, 2000, pp. 1-10.